

Nucleon elastic scattering in quark-diquark representation with springy Pomeron

V.M. Grichine^a

Lebedev Physical Institute, Moscow, Russia

Received: date / Revised version: date

Abstract. A model for elastic scattering of nucleons (and anti-nucleons) based on the quark-diquark representation of the nucleon with springy Pomeron, providing increased real part of the scattering amplitude, is developed. The model predictions are compared with experimental data for the differential elastic cross-sections of nucleons in the energy range from few GeV up to 7 TeV using available databases.

PACS. 4 1.60.Bq , 29.40.Ka

1 Introduction

The quark-diquark (qQ-) model for description of the proton-proton elastic scattering proposed in [1] was recently updated and compared with experimental data in [2]. Fig. 1 shows the differential cross-section of proton-proton elastic scattering corresponding to the total energy in the center of mass system, $\sqrt{s}=7$ TeV. The curve corresponds to the qQ-model [2] with the standard Pomeron parametrization:

$$\exp \left\{ \tilde{\alpha} \left[\ln \frac{s}{s_o} - \frac{i\pi}{2} \right] \right\}, \quad (1)$$

where the Pomeron trajectory slope $\tilde{\alpha}=0.15$ GeV⁻² and the term $-i\pi/2$ defines the scattering amplitude real part of the qQ-model [2] ($s_o=1$ GeV²; we use units: $\hbar = c = 1$). It is seen that the curve overestimates the dip value, and the reason is that the scattering amplitude real part value is not big enough.

The picture here is similar to the elastic scattering of hadrons on nuclei. Fig. 2 shows the differential hadron elastic scattering cross-sections of protons with the energy 1 GeV on lead versus the polar scattering angle [4]. The pure diffuse diffraction model proposed in [4] does not describe the minimum regions of the differential cross-section. If we add, however, the Coulomb amplitude, which increases the scattering amplitude real part, the model becomes to be more close to the experimental data. The Coulomb amplitude can increase the scattering amplitude real part for heavy nuclei with high atomic number only. In the case of nucleons one should modify directly the hadronic amplitude. Therefore one can assume, that if we increase the imaginary part of the Pomeron parametriza-

tion (1), i.e. apply:

$$\exp \left\{ \tilde{\alpha} \left[\ln \frac{s}{s_o} - \alpha_p \frac{i\pi}{2} \right] \right\}, \quad (2)$$

with the empirical parameter, $|\alpha_p| > 1$, which can be named as the Pomeron elasticity, we can improve the description of the hadron-hadron elastic scattering. This modification is proposed in the current paper together with an extension of the qQ-model to the case of the elastic scattering of different nucleons (and even hadrons).

We discuss below the main features of the extended qQ-model suitable for numerical calculations of elastic scattering of different nucleons and provide comparisons with the experimental data for the pp , np , and $\bar{p}p$ elastic differential cross-section in the energy range from few GeV up to 7 TeV in the center of mass system.

2 Quark-diquark model for nucleon-nucleon elastic scattering

The nucleon-nucleon differential elastic cross-section, $d\sigma_{el}/dt$, can be expressed in terms of the scattering amplitude $F(s, t)$:

$$\frac{d\sigma_{el}}{dt} = \frac{\pi}{p^2} |F(s, t)|^2, \quad (3)$$

where p is the nucleon momentum in the center of mass system, and t is the four-momentum transfer squared.

We consider here an extension of the model [2] describing the elastic scattering of two different nucleons. The first nucleon consists of quark (index 1), diquark (2), and the second one consists of quark (3) and diquark (4). The model [2] limits the consideration of the scattering amplitude by contributions from one- and two-Pomeron exchanges between quark-quark (1-3), diquark-diquark (2-4)

^a e-mail: Vladimir.Grichine@cern.ch

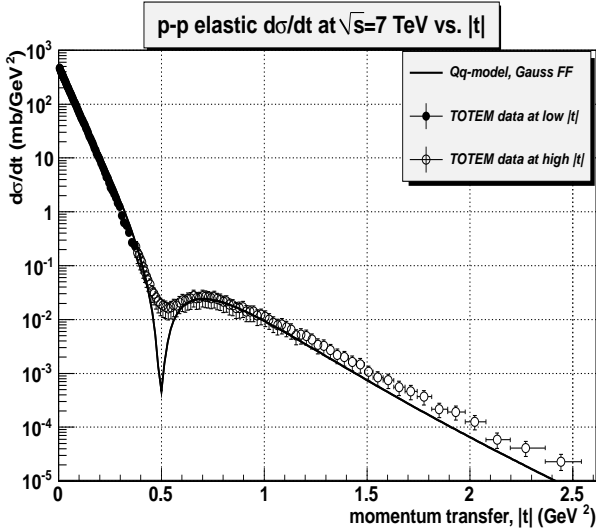


Fig. 1. The proton-proton differential elastic cross-section versus $|t|$ at $\sqrt{s} = 7$ TeV. The curve is the prediction of quark-diquark model [2]. The open and closed circles are the LHC TOTEM experimental data from [3].

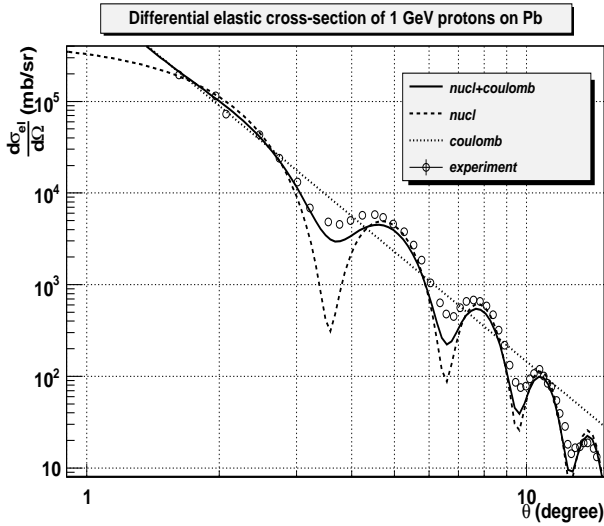


Fig. 2. The differential hadron elastic scattering cross-sections of protons with the energy 1 GeV on lead versus the polar scattering angle [4]. The curves show the pure nuclear (dash-dash) and with the Coulomb correction (solid) models. The dot-dot line corresponds to the pure electromagnetic Coulomb scattering. The open points are experimental data.

and two quark-diquark (1-4, 2-3). In this approximation $F(s, t)$ can be expressed as:

$$F(s, t) = F_1(s, t) - F_2(s, t) - F_3(s, t), \quad (4)$$

where $F_1(s, t)$ is the scattering amplitude with one-Pomeron exchange, while $F_2(s, t)$ corresponds to two-Pomeron exchanges between the nucleon constituents, quark and diquark, and $F_3(s, t)$ corresponds to two-Pomeron exchanges between the quark (or diquark) of one nucleon and the quark and the diquark of another nucleon at the same

time. The amplitude $F_1(s, t)$ reads:

$$F_1(s, t) = \frac{ip\sigma_{tot}(s)}{4\pi} [f_{13} + f_{14} + f_{23} + f_{24}], \quad (5)$$

$$f_{13} = B_{13} \exp[(\xi_{13} + \beta^2 \lambda + \delta^2 \eta)t],$$

$$f_{14} = B_{14} \exp[(\xi_{14} + \beta^2 \lambda + \gamma^2 \eta)t],$$

$$f_{23} = B_{23} \exp[(\xi_{23} + \alpha^2 \lambda + \delta^2 \eta)t],$$

$$f_{24} = B_{24} \exp[(\xi_{24} + \alpha^2 \lambda + \gamma^2 \eta)t],$$

where $\sigma_{tot}(s)$ is the total nucleon-nucleon cross-section. The coefficients B_{jk} , parametrize the quark-quark, diquark-diquark and quark-diquark cross-sections:

$$\sigma_{13} = B_{13}\sigma_{tot}(s), \quad \sigma_{24} = B_{24}\sigma_{tot}(s),$$

$$\sigma_{23} = B_{23}\sigma_{tot}(s), \quad \sigma_{14} = B_{14}\sigma_{tot}(s).$$

The model assumes the quark-diquark cross-section, $\sigma_{23} = \sigma_{14} = \sqrt{\sigma_{13}\sigma_{24}}$. The coefficients $\alpha = \gamma = 1/3$, and $\beta = \delta = 2/3$ correspond to the relative masses of quark and diquark in the nucleons. The parameters λ and η are equal to the the first and second nucleon radius squared divided by four, respectively.

The coefficients ξ_{jk} , ($j, k = 1, 2$) are derived taking into account the Gauss distribution of quark and diquark in nucleon together with the Pomeron parametrization discussed above in relation (2). They read:

$$\xi_{jk} = \frac{r_j^2 + r_k^2}{16} + \tilde{\alpha} \left[\ln \frac{s}{s_0} - \alpha_p \frac{i\pi}{2} \right]. \quad (6)$$

Here r_j, r_k are the quark or diquark radii. The quark and diquark radii r_1 (r_3) and r_2 (r_4) were found by the fitting of experimental data to be 0.173 and 0.316 of the corresponding nucleon radius, respectively.

The amplitudes $F_2(s, t)$ and $F_3(s, t)$ are:

$$F_2(s, t) = \frac{ip\sigma_{tot}^2(s)}{16\pi^2} [f_{13,24} + f_{14,23}], \quad (7)$$

$$f_{13,24} = \frac{B_{13}B_{24}}{\xi_{13} + \xi_{24} + \lambda + \eta} \exp \left\{ [\xi_{24} + \alpha^2 \lambda + \gamma^2 \eta - \frac{(\xi_{24} + \alpha \lambda + \gamma \eta)^2}{\xi_{13} + \xi_{24} + \lambda + \eta}] t \right\},$$

$$f_{14,23} = \frac{B_{14}B_{23}}{\xi_{14} + \xi_{23} + \lambda + \eta} \exp \left\{ [\xi_{23} + \alpha^2 \lambda + \delta^2 \eta - \frac{(\xi_{23} + \alpha \lambda + \delta \eta)^2}{\xi_{14} + \xi_{23} + \lambda + \eta}] t \right\},$$

and:

$$F_3(s, t) = \frac{ip\sigma_{tot}^2(s)}{32\pi^2} [f_{13,14} + f_{23,24} + f_{13,23} + f_{14,24}], \quad (8)$$

$$f_{13,14} = \frac{B_{13}B_{14}}{\xi_{13} + \xi_{14} + \eta} \exp \left\{ [\xi_{14} + \beta^2 \lambda + \gamma^2 \eta - \frac{(\xi_{14} + \gamma \eta)^2}{\xi_{13} + \xi_{14} + \eta}] t \right\},$$

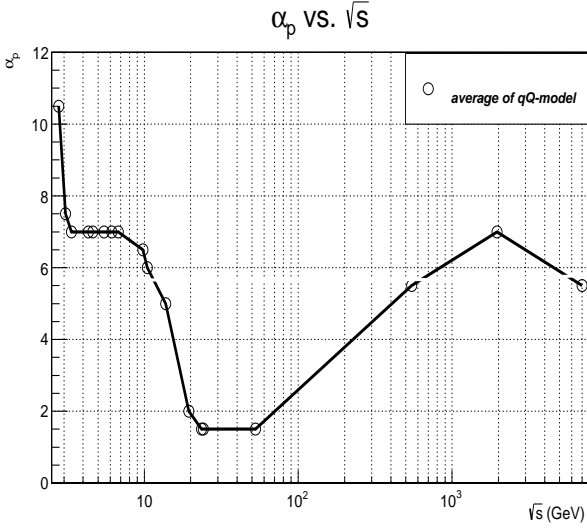


Fig. 3. The dependence of α_p versus the \sqrt{s} .

$$f_{23,24} = \frac{B_{23}B_{24}}{\xi_{23} + \xi_{24} + \eta} \exp \left\{ \left[\xi_{24} + \alpha^2 \lambda + \gamma^2 \eta - \frac{(\xi_{24} + \gamma \eta)^2}{\xi_{23} + \xi_{24} + \eta} \right] t \right\},$$

$$f_{13,23} = \frac{B_{13}B_{23}}{\xi_{13} + \xi_{23} + \lambda} \exp \left\{ \left[\xi_{23} + \alpha^2 \lambda + \delta^2 \eta - \frac{(\xi_{23} + \alpha \lambda)^2}{\xi_{13} + \xi_{23} + \lambda} \right] t \right\},$$

$$f_{14,24} = \frac{B_{14}B_{24}}{\xi_{14} + \xi_{24} + \lambda} \exp \left\{ \left[\xi_{24} + \alpha^2 \lambda + \beta^2 \eta - \frac{(\xi_{24} + \alpha \lambda)^2}{\xi_{14} + \xi_{24} + \lambda} \right] t \right\},$$

respectively.

To simplify the numerical calculations, one can assume that all nucleons involved to the elastic scattering have the same radius and the quark-quark and diquark-diquark cross-sections do not depend on the what quarks (u or d , as well as \bar{u} or \bar{d}) interact. Then the quark-quark cross-section, σ_{13} , the nucleon radius and the Pomeron elasticity, α_p , are the free parameters defining (together with $\sigma_{tot}(s)$) the s -dependence of the $d\sigma_{el}/dt$. The diquark-diquark cross-section, σ_{24} , and the parameter B_{24} are derived from the optical theorem, as it was discussed in [2]. The s -dependencies of the nucleon radius and the quark-quark cross-section are essentially the same as it was shown in [2]. The averaged s -dependence of the Pomeron elasticity, α_p is shown in fig. 3.

3 Comparison with experimental data

Fig. 4, 5, and 6 show the proton-proton differential elastic cross section at $\sqrt{s} = 7$ TeV versus $|t|$ and the antiproton-proton differential elastic cross-sections at, $\sqrt{s} = 1960$ GeV

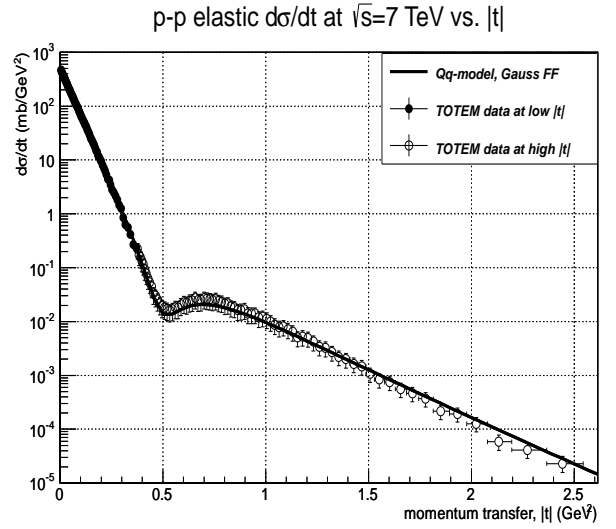


Fig. 4. The proton-proton differential elastic cross-section versus $|t|$ at $\sqrt{s} = 7$ TeV. The curve is the prediction of quark-diquark model with springy Pomeron. The open and closed circles are the LHC TOTEM experimental data from [3].

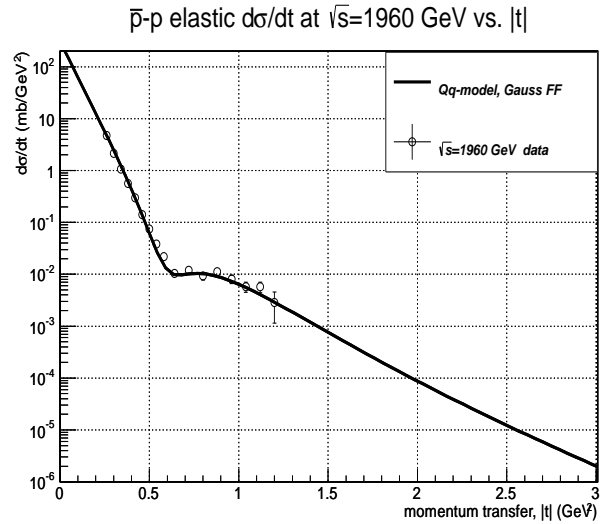


Fig. 5. The antiproton-proton differential elastic cross-section versus $|t|$ at $\sqrt{s} = 1960$ GeV. The curve is the prediction of our model. The open circles are the experimental data [5].

and $\sqrt{s} = 546$ GeV, respectively. The curves are the predictions of our model. We see that the proposed qQ -model with springy Pomeron describes reasonably the differential elastic cross sections of the antiproton-proton and proton-proton scattering in the TeV-region of energy.

Fig. 7 and 8 show the neutron-proton differential elastic cross sections at the neutron momentum in the laboratory system 100 and 9 GeV/c, respectively. Fig. 10 the proton-proton differential elastic cross-section versus $|t|$ at the proton momentum in the laboratory system 3 GeV/c. One can see the satisfactory agreement of the qQ -model with experimental data in the GeV-range of energy.

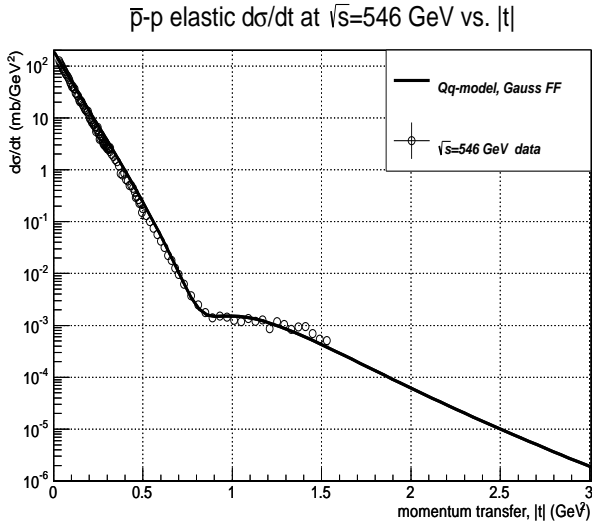


Fig. 6. The antiproton-proton differential elastic cross-section versus $|t|$ at $\sqrt{s} = 546$ GeV. The curve is the prediction of our model. The open circles are the experimental data [6].

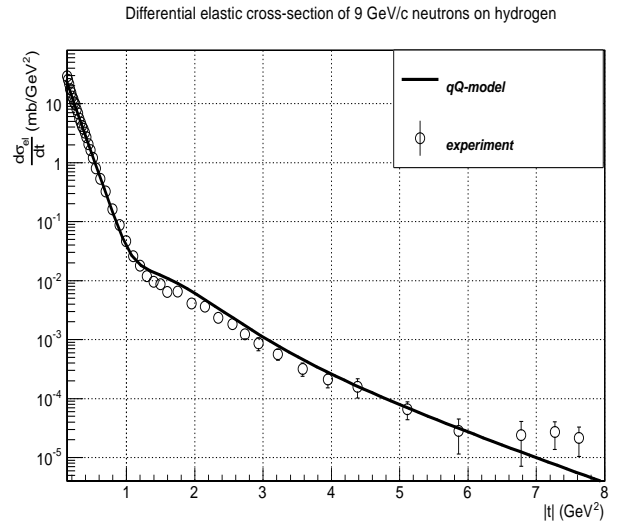


Fig. 8. The neutron-proton differential elastic cross-section versus $|t|$ at the neutron momentum in the laboratory system 9 GeV/c. The curve is the prediction of our model. The open circles are the experimental data [8].

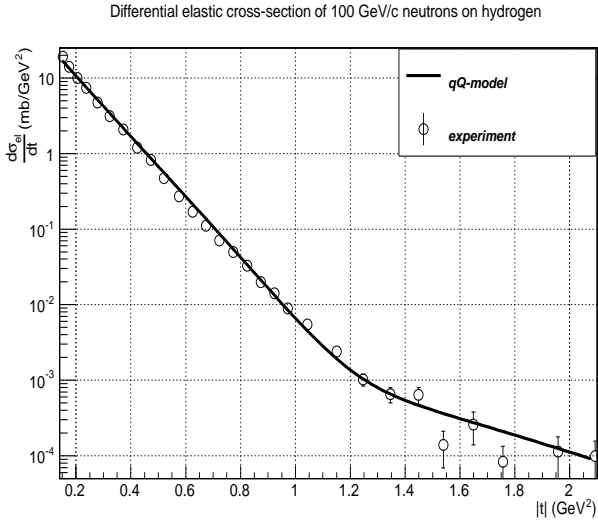


Fig. 7. The neutron-proton differential elastic cross-section versus $|t|$ at the neutron momentum in the laboratory system 100 GeV/c. The curve is the prediction of our model. The open circles are the experimental data [7].

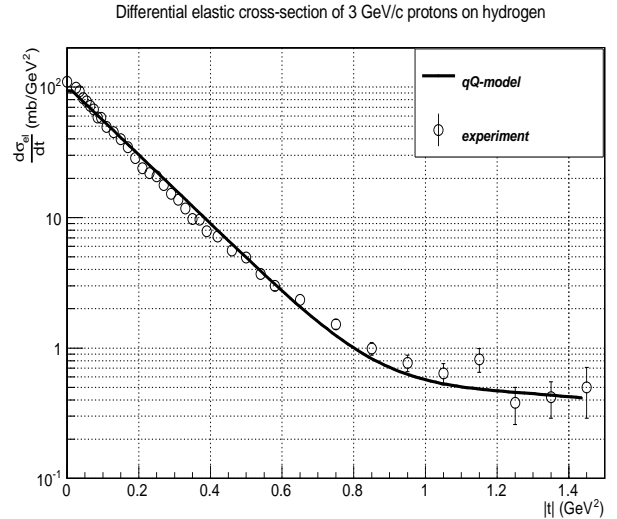


Fig. 9. The proton-proton differential elastic cross-section versus $|t|$ at the proton momentum in the laboratory system 3 GeV/c. The curve is the prediction of our model. The open circles are the experimental data [9].

4 Summary

We have considered the qQ -model of the nucleon-nucleon elastic scattering with springy Pomeron and compared it with experimental data. It was obtained reasonable description of the differential cross section of elastic pp $\bar{p}p$ and np scattering in a wide range of energies from few GeV to 7 TeV in the center of mass system. The dip position and its value of the $d\sigma_{el}/dt$ are in the satisfactory agreement with experimental data.

The qQ -model, in the framework of relations (5)-(8), can be easily generalized to the case of elastic scattering of mesons on nucleons or mesons on mesons. Fig. 10 shows

the $\pi^+ - p$ differential elastic cross-section versus $|t|$ at the π^+ momentum in the laboratory system 4.122 GeV/c, as an example of the qQ -model application to the case of meson-nucleon elastic scattering. The meson-nucleon elastic scattering in terms of the qQ -model with springy Pomeron will be reported in next paper.

Acknowledgment

The author is thankful to S. Bertolucci, S. Giani and M. Mangano for stimulating discussions and support. The

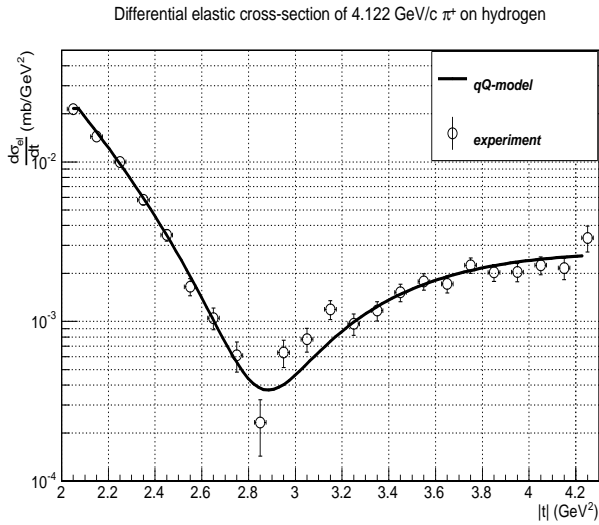


Fig. 10. The $\pi^+ - p$ differential elastic cross-section versus $|t|$ at the π^+ momentum in the laboratory system 4.122 GeV/c. The curve is the prediction of our model. The open circles are the experimental data [10].

meetings and e-mail communication with N. Starkov and N. Zotov were powerful for clarification of the qQ-model details. The work was also partly supported by the CERN-RAS Program of Fundamental Research at LHC.

References

1. V.A. Tsarev, *Lebedev Institute Reports*, **4** (1979) 12.
2. V.M. Grichine, N.I. Starkov and N.P. Zotov, *Eur. Phys. J.*, **C73** (2013) 23201;
3. G. Antchev et al. (TOTEM Collaboration), *Europhys. Lett.*, **95** (2011) 41001; *CERN-PH-EP-2012-239*.
4. V.M. Grichine, *Comp. Phys. Comm.*, **191** (2010) 921.
5. D0 Collaboration, *D0 Note 6056-CONF*.
6. M. Bozzo et al., *Phys. Letters*, **B147** (1984) 385; *ibid*, **B155** (1985) 197.
7. C.E. DeHaven, Jr. C.A. Ayre, H.R. Gustafson, et al., *Phys. Rev. Letters*, **41** (1978) 669.
8. J.L Stone, J.P. Shanowski, S.W. Gray, et al., *Phys. Rev. Letters*, **38** (1977) 1315.
9. I. Ambats, D.S. Ayres, R. Diebold, et al., *Phys. Rev.*, **D9** (1974) 1179.
10. K.A. Jenkins, C.E. Price, R. Klem, et al., *Phys. Rev. Letters*, **40** (1978) 425.